Engineering Notes

ENGINEERING NOTES are short manuscripts describing new developments or important results of a preliminary nature. These Notes cannot exceed 6 manuscript pages and 3 figures; a page of text may be substituted for a figure or vice versa. After informal review by the editors, they may be published within a few months of the date of receipt. Style requirements are the same as for regular contributions (see inside back cover).

Holographic Interferometric Mode Shape Patterns of Cored Mirrors

JACOB M. MILLER*
Itek Corp., Lexington, Mass.

Introduction

NEW measurement techniques are required for 30-to 120-in.-diam, cored-construction lens and mirror telescope systems. When vibration data are measured, the high stiffness/weight ratios of the large mirrors present problems. During initial attempts to monitor vibration patterns by using conventional piezo-electric instrumentation, problems arose because of low-level response at resonance (e.g., 0.01 g and 60×10^{-6} in. at 400 Hz). To monitor response for vibration mode pattern definition accurately, a better technique was required. Use of holographic interferometry to determine deflection patterns of cored mirrors loaded mechanically and thermally indicated that the same basic techniques could be used to define vibratory motions. In subsequent investigations, vibration mode patterns of large cored-construction mirrors, for the first time, were obtained by holographic interferometry. With holographic interferometry (real-time and time-averaged), amplitudes as low as 24×10^{-6} in. were observed, providing mode patterns that resulted in meaningful information. Although other investigators have reported obtaining vibration mode shapes by dynamic holography for beams and plates,[3-6] no previous dynamic holograms for large mirrors have been reported.

Two of the main advantages of dynamic holography are: 1) absence of vibration-measuring instruments on the specimen; (added inertias can alter the mode shapes per Ref. 6); 2) ability to sense motions too small ($<60 \times 10^{-6}$ in. and $<0.01\ g$) to be sensed by conventional instrumentation.

Description of Holographic Apparatus

The theoretical basis of holographic interferometry is discussed in Refs. 1–3. Figure 1 illustrates the optical and photographic apparatus used in the present investigations. One of the interfering light beams is the reflected reference beam, and the other beam is reflected from the object whose motion is to be measured. Differences in optical path lengths between the two light beams cause fringe patterns to be stored on the hologram plate. It was found that both the time-average and real-time techniques could be used effectively to obtain fringe patterns. The fringe pattern could then be converted to a deflection mode pattern by noting the location of equal brightness fringes which correspond to equal deflection lines in the vibration mode shapes.

A Ling 203 electrodynamic shaker was used for vibration excitation of the cored mirrors. The shaker was connected physically to the mirrors (called lightweights) in a variety of ways to evaluate the effects of such connections. The support conditions were varied by removing the felt pads in each support. The pads appeared to act as a spring between the mirror and support structure reactive forces. The resonances of the mirror (as a rigid body)-pads system produced no circular fringes across the mirror. Thus, these resonances did not affect the observed circular fringe patterns. The damping effect of the pads appeared to be small since the frequency was the same with and without pads. The support conditions are such that a free-free condition occurs during oscillations when felt pads are used. The effects of the pads are discussed below.

Interpretation of Dynamic Holograms

The reconstructed images from the vibrating lightweight mirrors were photographed by the system just described. The circular fringe patterns shown in Fig. 2 indicate that the three-point static support was not fully effective as a dynamic support, and that the large lightweight mirror was vibrating in an almost free-free mode. This interpretation is based on the fact that[7] free-free vibrations have circular mode shapes whereas three-point-supported vibrations have tri-angularized mode shapes. For further verification, for three-point supports analytic mode shapes were determined at 643 Hz and at 1,626 Hz for free supports. Figures 3 and 4 are the photographs of the fringe patterns for the 31-in. diam Plexiglas mirrors. One has a triangular core pattern and the other has a hexagonal core pattern. Because the photographs show fringes surrounding the deflection nodes at the supports, predicted by classical analysis, it is concluded that the mount system used was effective as a three-point dynamic mount. Node regions of no motion for second vibration modes at about $r/2$ are expected but the distorted node region obtained indicated that shear transferral through the core, local effects, and/or rigid tilting may have occurred. Holes of $\frac{3}{4}$ in. and $1\frac{1}{2}$ in. were also drilled into the back faces of the

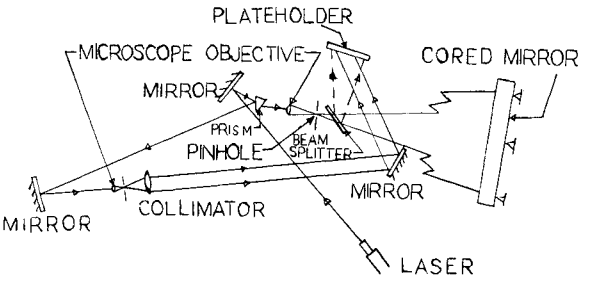

Fig. 1 Schematic of dynamic holography system.

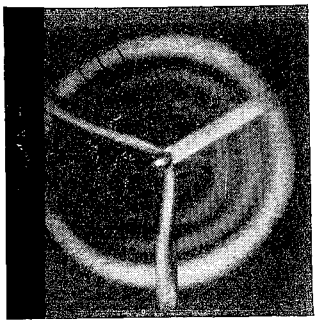

Fig. 2 Reconstructed 960 Hz beam, mirror resting on pads.

Presented as Paper 71-180 at the AIAA 9th Aerospace Sciences Meeting, New York, January 25–27, 1971; submitted February 16, 1971; revision received October 4, 1971.

Index categories: Structural Dynamic Analysis; Structural Composite Materials (Including Coatings); Research Facilities and Instrumentation.

* Staff Aeronautical Engineer; also Graduate Student, Northeastern University, Boston, Mass.; presently Senior Principal Development Engineer, Honeywell Radiation Center, Lexington, Mass.

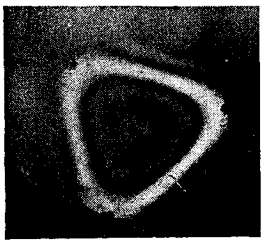

Fig. 3 Fringe pattern at 490 Hz resonance of 31-in.-diam triangular cored mirror.

Fig. 4 Fringe pattern at 450 Hz resonance of 31-in.-diam hexagonal cored mirror.

triangular and hexagonal core mirrors. Dynamic holograms were made of the mirrors with the holes. The data indicated that the same mode shapes occurred and the resonant frequencies were reduced by 5 to 10%.

References

[1] Gabor, D., "Microscopy By Reconstructed Wavefronts," *Proceedings of the Royal Society (London)*, Ser. A, Vol. 197, July 1949, pp. 454–487.

[2] Leith, E. N. and Upatnieks, J., "Wavefront Reconstruction with Diffused Illumination and Three-Dimensional Objects," *Journal of Optical Society of America*, Vol. 54, Nov. 1964, pp. 1295–1301.

[3] Stetson, K. A. and Powell, R. L., "Interferometric Holographic Evaluation and Realtime Vibration Analysis of Diffuse Objects," *Journal of Optical Society of America*, (letters), Vol. 55, Aug. 1965, pp. 1694–1695.

[4] Hildebrand, B. P. and Haines, K. A., "Multiple-Wavelength and Multiple-Source Holography Applied to Contour Generation," *Journal of Optical Society of America*, Vol. 57, Feb. 1967, pp. 155–162.

[5] Leith, E. N. and Upatnieks, J., "Imagery With Coherent Optics," *Society of Photo-Optical Instrumentation Engineering Journal*, Vol. 3, April 1965.

[6] Barnett, N. E., "Progress Report on Vibration Analysis by Holographic Interferometry," Paper WA17, Oct. 1967, *Annual Meeting of Optical Society of America*, Detroit, Mich.

[7] Harris, C. M. and Crede, C. E., "Shock and Vibration Handbook," Vol. 1, *McGraw-Hill*, New York, 1961, pp. 7–32.

Shock-Wave, Turbulent Boundary-Layer Interaction on a Blunted Compression Surface

WILLIAM C. ROSE,* HELMER L. NIELSEN,† AND EARL C. WATSON‡

NASA Ames Research Center, Moffett Field, Calif.

* Received June 7, 1971. Research Scientist. Member AIAA.

† Professor, Department of Mechanical Engineering, San Jose State College, San Jose, Calif. NASA-ASEE Summer Fellow, 1970. Member AIAA.

‡ Research Scientist. Member AIAA.

Introduction

THE problem of analyzing the internal flow in inlets for aircraft that will fly at hypersonic speeds in the atmosphere is of current interest. The requirement for surfaces on such aircraft to have blunted leading edges has been noted.[1] The presence of a blunt leading edge produces a curved bow shock wave and a resulting downstream flowfield with nonzero vorticity. Thus, the viscous boundary layer (the primary concern here is with a turbulent layer) that develops on the surface may be significantly different from one that develops with the vorticity external to the boundary layer equal to zero. It is of paramount interest in the analysis and design of inlet systems to know what effect this nonzero vorticity flowfield and the resulting differences in the turbulent boundary layer will have on shock-wave boundary-layer interactions that occur inside the inlet.

Analyses proposed to treat interactions between shock waves and turbulent boundary layers have used the assumption of zero vorticity external to the boundary layer and have been limited to flows on flat plates[2] or to flows in a zero pressure gradient, axisymmetric environment.[3] The method of Ref. 4 was applied to a turbulent flow on a flat plate with no external vorticity; however no assumption in that method restricts its use to that class of flows. This Note describes the application of the method of Ref. 4 to analyze a shock wave interacting with a turbulent boundary layer on a blunted compression surface. Only the details of the method of Ref. 4 that specifically apply to the case under consideration are discussed.

Discussion

The experimental investigation described in Ref. 1 studied the effect of leading-edge bluntness on the flowfield downstream of the bow shock wave, including the interaction of a shock wave with the boundary layer. The investigation was carried out on a two-dimensional configuration and included studies of both laminar and turbulent boundary layers. One set of data for a turbulent boundary layer from that study has been singled out for detailed examination in the present paper. The data set was selected to test the ability of the method of Ref. 4 to describe features of shock-wave boundary-layer interactions that were not included in the cases studied in Ref. 4. For example, the selected data exhibit a boundary-layer separation as well as large vorticity contiguous to the viscous boundary layer.

A schematic of the model used in the experiments is shown in Fig. 1. The leading edge radius is 4.77 mm and the shock wave generator setting, α_G, is 6°. Details of the compression surface curvature and alignment with the freestream flow are

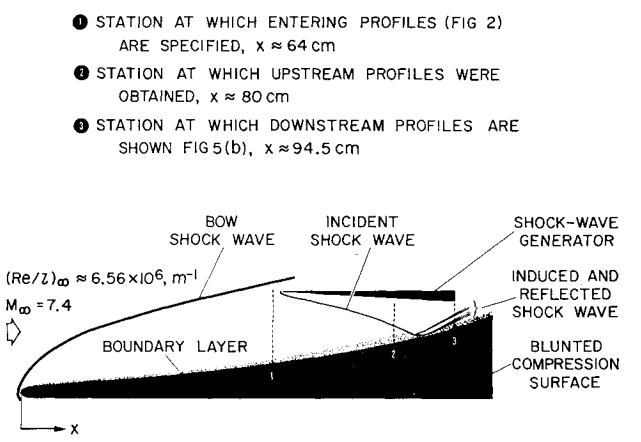

Fig. 1 Schematic of experimental model showing locations of survey stations.